

OpenLex3D: A New Evaluation Benchmark for Open-Vocabulary 3D Scene Representations

Christina Kassab^{*1}, Sacha Morin^{*2,4}, Martin Büchner^{*3}, Matías Mattamala¹,
Kumaraditya Gupta^{2,4}, Abhinav Valada³, Liam Paull^{2,4,5}, Maurice Fallon¹

¹University of Oxford ²Université de Montréal ³University of Freiburg
⁴Mila - Quebec AI Institute ⁵Canada CIFAR AI Chair

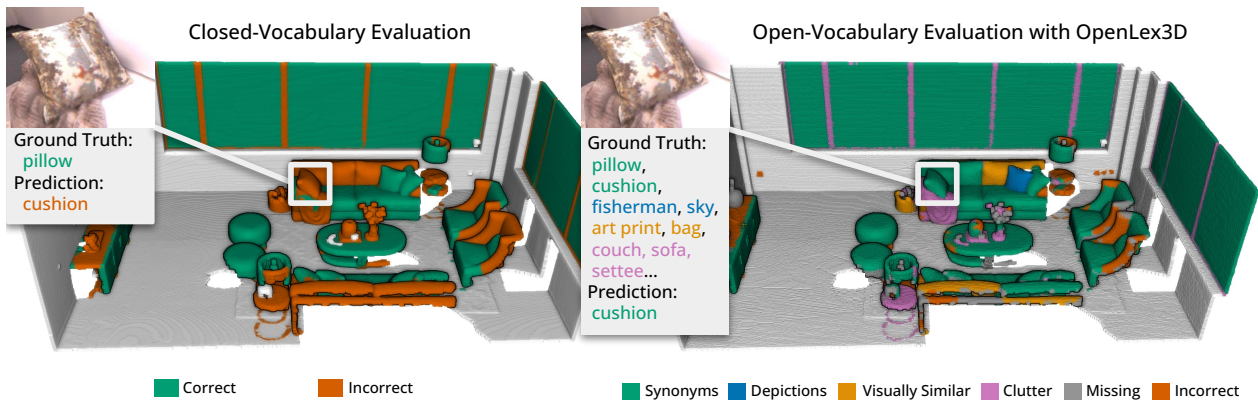


Figure 1: The OpenLex3D evaluation benchmark enables detailed analysis of open-vocabulary 3D scene representations compared to closed-vocabulary evaluation methods. We compare the same open-vocabulary representation when assessed under closed-vocabulary semantics (left) and using OpenLex3D labels (right). In contrast to closed-vocabulary methods where a prediction must match the exact ground truth label, OpenLex3D provides a manifold of label categories of varying precision: *synonyms* being the most precise; *depictions*, which include, e.g., printed images on objects; *visually similar*, which refer to objects with comparable appearance; and *clutter*, which accounts for label perturbation due to imprecise segmentation.

Abstract

3D scene understanding has been transformed by open-vocabulary language models that enable interaction via natural language. However, the evaluation of these representations is limited to closed-set semantics that do not capture the richness of language. This work presents OpenLex3D, a dedicated benchmark to evaluate 3D open-vocabulary scene representations. OpenLex3D provides entirely new label annotations for 23 scenes from Replica, ScanNet++, and HM3D, which capture real-world linguistic variability by introducing synonymical object categories and additional nuanced descriptions. By introducing an open-set 3D semantic segmentation task and an object retrieval task, we provide insights on feature precision, segmentation, and downstream capabilities. We evaluate various existing 3D open-vocabulary methods on OpenLex3D, showcasing failure cases, and avenues for improvement. The benchmark is publicly available at: <https://openlex3d.github.io>.

1. Introduction

3D scene understanding is a key capability enabling embodied agents to perceive, interpret, and interact with the physical world. An effective scene representation should generalize across diverse indoor and outdoor environments, supporting a broad range of objects and affordances [4]. The introduction of visual-language models such as CLIP [23] and LLaVa [17] has transformed this field, allowing objects to be labeled with descriptive features or captions rather than being constrained to closed-set semantics. This has motivated the development of methods that can leverage the open-vocabulary capabilities of these models to develop more general and versatile scene understanding systems [8, 11, 14, 16, 18, 22, 30, 33].

Evaluating fixed-class models is relatively straightforward—the predicted class label of each point-

wise prediction can be compared with the point’s ground truth label as shown in Fig. 1. In contrast, assessing the performance of open-vocabulary models is more challenging and is not yet well defined by a benchmark. Published works on open-vocabulary representations [30, 33] have typically used closed-set semantic segmentation labels and metrics—despite this underlying mismatch. This defeats the purpose and flexibility of open-vocabulary predictions by constraining the model assessment to a limited set of evaluation classes [21, 30].

Furthermore, relying on evaluation benchmarks designed for fixed-class semantics overlooks the nuance of real-world language labeling, which rarely lends itself to binary classification. Examples of this include synonyms or other descriptive words that encompass more general classes. For example, a couch might also be referred to as a “sofa” or “seating”. Prior work has proposed using existing ontologies like WordNet (a large English language lexical database) [20] to mitigate these ambiguities in language benchmarks, though differentiating between *similarities* and *associations* remains an open question [10].

Some open-vocabulary challenges have sought to evaluate performance in a *functional* manner, by focusing on tasks such as visual question answering and object retrieval [5, 6, 36]. However, methods that focus on querying specific prompts will fail to evaluate the full 3D representation and offer limited insights into overall limitations.

In this work, we aim to overcome these limitations by introducing OpenLex3D, a novel benchmark that evaluates open-vocabulary scene representation methods. OpenLex3D introduces a procedure built on *four different label categories* of description accuracy: *synonyms*, *depictions*, *visual similarity*, and *clutter*. These categories evaluate the performance of a method in capturing the correct class (*synonyms*) while also quantifying different degrees of misclassifications. Our benchmark is implemented by relabeling three widely-used indoor RGB-D datasets with a new set of human-annotated ground truth labels. We define two evaluation tasks to quantify the performance of open-vocabulary scene representation methods. Our contributions are:

Open-set Category Labels. We introduce a new labeling scheme where each object has multiple free-form text labels organized into four categories with different accuracy levels of linguistic description.

Dataset. We provide OpenLex3D labels for 23 scenes from Replica [29], Scannet++ [37] and Habitat-Matterport 3D [24]. Each object has been reviewed by four human annotators, resulting in an average of 11 labels per object.

Two Evaluation Tasks. We provide evaluation on two tasks using the OpenLex3D dataset: semantic segmentation and object retrieval given a text query. We introduce two novel open-set metrics for segmentation and an extended query list for object retrieval. We evaluate state-of-the-art 3D

open-vocabulary methods on both tasks.

Benchmark Toolkit. We make the OpenLex3D toolkit and ground truth data publicly available at: <https://openlex3d.github.io>.

2. Related Work

2.1. Open-Vocabulary Scene Representations

The recent development of Visual-Language Models (VLMs) has opened up new possibilities for building semantic scene representations that can be interacted with using natural language. This has motivated the integration of VLMs into *object-centric* and *dense* map representations.

Object-centric representations explicitly factorize scene geometry as a set of 3D objects and represent semantic information as object-level open-vocabulary features from vision-language encoders such as CLIP [23]. Methods typically derive object features by fusing features from multiple views using various strategies [13]. This makes them a compact representation for embodied AI applications that involve object-level understanding and interaction, such as object retrieval.

Methods such as OpenMask3D [30] first determine candidate objects using instance segmentation and then assign CLIP embeddings to each object instance. A similar approach has been followed by open-vocabulary scene graph methods, which use the object vocabulary instances as graph nodes, and then extend the nodes with edges that encode relationships or affordances, which can also be obtained by means of a VLM such as LLaVa [17] or GPT-4V [35]. Open-vocabulary scene graphs include ConceptGraphs [8], HOV-SG [33], Clio [19], and Open3DSG [16].

Dense representations instead produce dense open-vocabulary feature embeddings for every point in a scene. The underlying geometric representations include voxels, point clouds, or more recently, neural fields or Gaussian splats. These methods include OpenScene [21] and ConceptFusion [12] and produce dense point cloud maps, where each point stores an open-vocabulary embedding.

More recent work uses radiance fields to encode open-vocabulary features including LERF [14], VL-Fields [31], and CLIP-Fields [28]. This enables the rendering of photo realistic novel views with pixel-wise open-vocabulary feature labeling. Similar ideas have also been used with 3D Gaussian representations, namely LangSplat [22], semantic Gaussians [9], and OpenGaussian [34].

2.2. Evaluating Open-Vocabulary Representations

Recent works focus on two tasks to evaluate open-vocabulary 3D representations: semantic segmentation and object retrieval given a text query.

Semantic Segmentation. Open-vocabulary 3D representations can achieve class prediction by comparing their features with a *prompt list* to output the top-ranking class for every point, and then rely on conventional segmentation metrics for evaluation. Common datasets include ScanNet (20 classes) [3] and Replica (88 classes) [29]. While showcasing impressive zero-shot capabilities, this approach biases the results as it constrains the space of predicted labels to valid labels only. Furthermore, this approach does not take into account the nuance of real-world object labeling, where multiple correct labels are possible.

In contrast, OpenLex3D overcomes these challenges by providing an extensive set of human-annotated labels for every object. These labels account for natural variability in language and are categorized in terms of description specificity. We complement our dataset with two novel segmentation metrics to explore both the top predictions and the complete ranking of the prompt list.

Object Retrieval. An object-centric representation can serve as a retrieval system by returning objects sharing similar features with a user-specified text query. We treat retrieval as an instance segmentation task while another line of work focuses on bounding-box regression [2, 32]. The flexibility of the task makes it challenging to automate evaluation, and previous query results do not cover all scene objects. ConceptGraphs [8] evaluates recall for 60 queries, while OpenScene [21] visually verifies retrieval results for 11 classes. Automated evaluation is possible when narrowing the scope of the queries to class labels [18, 30] at the cost of query diversity. The first OpenSun3D [6] workshop challenge provides replicable retrieval evaluation on multiple scenes but is restricted to 25 queries.

In comparison, we leverage the OpenLex3D category labels to procedurally generate hundreds of queries per scene as part of an automated benchmark. Our queries cover all scene objects and include specific information such as motifs, cultural references and brands.

3. The OpenLex3D Benchmark

3.1. Benchmark Design

Our benchmark aims to provide a comprehensive evaluation of 3D scene representations. To achieve this, we propose to change the goal of scene segmentation from determining a single correct label per object, to *determining a descriptive category* instead. In our benchmark each category is defined by a larger set of possible labels that describe an object with different levels of specificity. The categories are arranged hierarchically, with the top category containing the most specific labels relative to the target object, while the lowest category includes the least specific labels.

This structured approach enables us to define potential classification failure cases of 3D representations and to an-

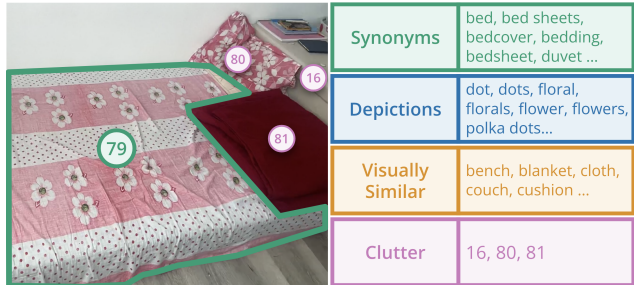


Figure 2: **OpenLex3D augmented labels example from ScanNet++** [37]. We provide not only synonyms for the object (bed sheet, duvet) but also labels for various potential failure cases, including depictions visible on the target object (e.g., flower prints), visually similar objects (e.g., blanket), and surrounding clutter (indicated by the ids of the neighboring objects).

alyze how and why they occur. The four categories we consider, in decreasing order of description accuracy, are:

Synonyms. This category includes the primary labels for the target object as well as any other equally valid label. For instance, “glasses” and “spectacles”.

Depictions. Labels in this category describe any images or patterns depicted on the target object. For example, if a pillow features an image of a tree, the label “tree” would fall under this category.

Visually Similar. This includes objects that appear to be visually similar to the target objects and are likely to be confused for it. For example, visually similar terms for “glasses” could include “sunglasses” or “goggles”.

Clutter. This category covers any nearby or surrounding objects. Surrounding object features may “leak” into the features of interest due to 1) co-visibility in the same RGB frames and/or 2) incorrect merging in object-centric representations. This is the only category not defined by word labels but object IDs pointing to the surrounding objects.

An example of these categories is shown in Fig. 2. An ideal 3D scene representation would generate predictions that fall exclusively under the *synonym* category. However, in practice, most representations would produce predictions distributed across all four categories, therefore providing insights into different failure modes. For example, a representation that yields many predictions in the *clutter* category may indicate problems such as under-segmentation or merging of objects such as small items on tables. Conversely, a representation with many predictions in the *visually similar* category might point to issues with the open-vocabulary model itself or the feature-merging strategy used by the map construction method, suggesting that the features are less distinctive and fail to differentiate between visually similar objects.

We use nouns (including multiple word labels such as “sofa cushion”) for our ground truth categories to reduce the ambiguities of sentences and captions. For instance, sentence embedding models [25], are sensitive to variations

in word order and struggle to distinguish between sentences with similar structures but different meanings. By using diverse nouns we can still capture semantic similarities without introducing such challenges.

3.2. Label Acquisition and Processing

3.2.1 Datasets

To implement the benchmark, we create an entirely new set of semantic labels for three prominent RGB-D datasets:

Replica [29] consists of a set of high-quality reconstructions of indoor spaces, including offices, bedrooms, and living spaces. We use eight scenes (*room0-room2* and *office0-office4*) and utilize the camera trajectories provided by NICE-SLAM [38].

ScanNet++ [37] is a large-scale dataset of a variety of real indoor scenes. Each scene provides laser scanner-registered images from a DSLR camera and RGB-D streams from an iPhone. We use the RGB-D iPhone images, along with their associated poses (metrically-scaled COLMAP [27] trajectories) from eight scenes.

HM3D [24] consists of 1000 high-resolution 3D scans of building-scale residential, commercial, and civic spaces. We use the trajectories generated by HOV-SG [33] and obtain RGB-D images as well as semantic ground truth across seven scenes of the *Habitat-Matterport 3D Semantics* split.

Supp. Sec. 8 provides more details about the selected scenes, as well as their specific IDs within each dataset.

3.2.2 Annotation Process

We had human annotators produce extended label sets for every ground truth object available on each scene of the datasets. The annotators used the *segments.ai* web labeling interface. Fig. 3 illustrates an example of the interface when labeling an object of the Replica dataset.

To generate the labeling data, we first obtained a set of representative images for each ground truth object instance using a method similar to that described in OpenMask3D [30]. For each object instance in the ground truth point cloud, we projected its 3D points into every image of the scene where the instance was visible. These projected 2D points were used to define a bounding box that encloses the object in the image. Additionally, we used the projected points to generate a Segment Anything (SAM) [15] mask, which provided clearer guidance for the annotator on the object to be labeled.

Our annotators were from three different countries and have a variety of backgrounds and professions. We recruited them directly rather than relying on third party platforms such as Amazon Mechanical Turk (MTurk). Studies have shown that online labeling platforms can suffer from significant errors. In a paper analyzing MTurk [26], be-

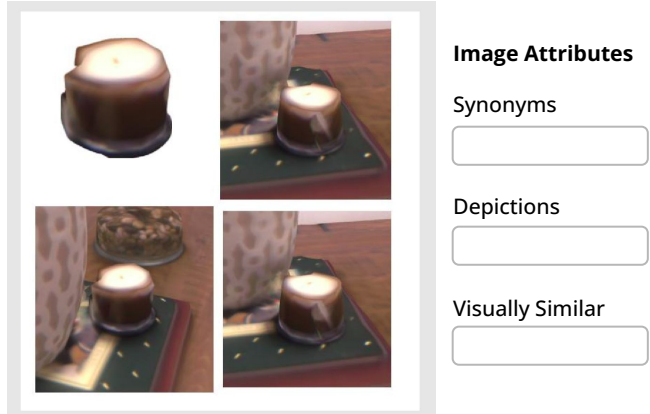


Figure 3: The *segments.ai* web interface showing an example provided image. The top left image is segmented using SAM [15] and aims to highlight the intended object for labeling more clearly to the annotator. The other images provide additional context.

tween 22.8% to 44.8% of images were labeled incorrectly and an additional 20.1% were marked as spam.

The annotators were required to fill in responses for the first three categories only (*synonyms*, *depictions*, and *visually similar*), and each object in every scene was labeled by four different annotators. The full instructions given to the annotators are included in Supp. Sec. 9. The *clutter* category was filled in post-processing after the annotation process (see Sec. 3.2.3).

3.2.3 Label Post-processing

After obtaining the labels, we curated them to correct spelling errors and eliminate invalid responses. The reviewing process followed these conventions: First, if the same label occurred in multiple categories, it was assigned to the lowest (least specific) category. Second, if there was significant disagreement in the synonyms category for the target object, the object was kept but flagged as “ambiguous” to indicate that it was difficult to recognize. Third, variations such as plurals and differences in spacing were permitted and remained unaltered (e.g., “shelves” and “shelf” or “counter top” and “countertop”).

The *clutter* category was filled in after the label curation. For each object in the scene, we identified nearby or surrounding objects based on their Intersection over Union (IoU). We used the Objectron [1] implementation to estimate bounding boxes and compute the IoU. Any neighboring objects with an IoU greater than 0 with the target object were assigned to the *clutter* category.

3.3. Evaluation Methodology

We propose two tasks to evaluate open-vocabulary 3D scene representation methods: a semantic segmentation task and an object retrieval task. The first task tests the accuracy

of the method in describing different objects in the scene, the latter assesses whether it can identify and segment all instances that best match a given query.

Both tasks are evaluated in 3D, requiring the benchmarked methods to either output a 3D point cloud along with language-aligned features (e.g., CLIP) for each point (for dense representations), or an instance-segmented point cloud with corresponding object-level open-vocabulary features (for object-centric representations). The object retrieval task only supports object-centric methods.

3.3.1 Task 1: Open-Set Semantic Segmentation

In the first task, we evaluate the open-vocabulary features (dense or per-object) stored in a representation using our category-based ground truth. This is achieved by determining the text-feature similarity of the features with a dataset-specific evaluation prompt list. This is achieved by computing the cosine similarity of the features against the prompt list embeddings. The prompt lists we introduce in OpenLex3D are built from unique labels across all categories and scenes in each dataset, containing between 1,000 and 3,000 unique words. This mitigates the problem of positive bias toward the correct labels [13]. To evaluate the performance of the 3D representation, we introduce two metrics:

Top-N IoU at Category. This metric characterizes the proportion of objects $o \in \mathcal{O}$ in a scene that are correctly classified into a particular category C . We define it as:

$$\text{IoU}^C = \frac{\sum_{o \in \mathcal{O}} \frac{TP_o^C}{n_o}}{\sum_{o \in \mathcal{O}} \left(\frac{TP_o}{n_o} + \frac{FP_o}{n_o} + \frac{FN_o}{n_o} \right)}, \quad (1)$$

where TP_o^C is the number of true positive points in category C ; TP_o , FP_o , and FN_o are the number of true positive, false positive and false negative points for all categories, normalized by the number of points of the object n_o .

To compute these quantities, we consider a predicted point label as a match for category C if any of the *top-N* responses of the text-feature similarity feature a label in category C (see Fig. 4a). This helps to mitigate any inconsistencies in the ground truth labels. If any of the top-N labels belong to the *synonyms* category, the point is classified as a *synonym*. If none of the top-N labels is a *synonym*, the point is assigned to the next highest-ranking category, *depictions*, as outlined in Sec. 3.1. The imposed ordering of the categories reflects the precision of the labels in describing the target object, with *synonyms* being the most precise and *visually similar* being the least. A point is classified as *clutter* if it does not fit into any of the previous categories but shares a label with any category of a neighboring object. If no labels in the top-N match any predefined category, the

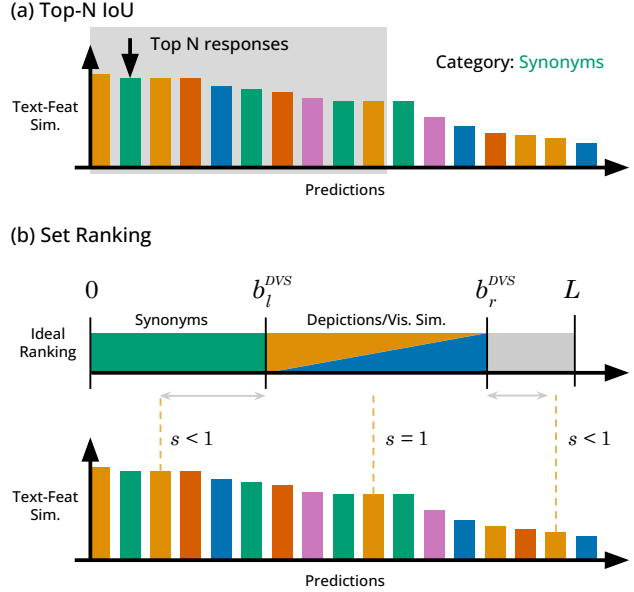


Figure 4: **Top-N IoU and Set Ranking metrics illustration.** (a) Top-N IoU measures whether any of the top-N responses contain a label from category C. (b) Set Ranking evaluates the ranking of responses, assessing how closely the predicted rankings align with ideal rankings of categories.

point is labeled as *incorrect*. Any points in the ground truth point cloud that have no corresponding points in the predicted cloud are labeled as *missing*.

Set Ranking. Our second metric assesses the distribution of the text-feature similarity of each point in the scene representation. For this, we quantify the mismatch of the responses when compared against an *ideal ranking* of category sets. We establish *synonyms* (S) as the first-rank set, while *depictions* and *visually similar* are considered as a joint second-rank set (DVS). The size of the sets is determined by the number of corresponding labels in the ground truth categories for each point. An example is shown in Fig. 4(b). Our proposed metric is computed for each point p in the predicted point cloud \mathcal{P} , using the full text-feature similarity predictions per point. We first sort the predictions according to the ideal set ranking (*synonyms* first, then *depictions* and *visually similar*). We obtain left and right ranking bounds for each set, b_l^C and b_r^C , where C denotes the category set (S or DVS). We then compute a *rank score* s_i for each prediction i , as a function of its rank r_i :

$$s(r_i) = \min \left(1 + \min \left(0, \frac{r_i - b_l^C}{b_l^C} \right), 1 - \max \left(0, \frac{r_i - b_r^C}{L - b_r^C} \right) \right), \quad (2)$$

where L denotes the total number of predictions in the text-feature similarity (given by the evaluation prompt list). If the prediction falls in the right category set, we define $s(r_i) = 1.0$, and $s(r_i) < 1.0$ otherwise. The rank scores

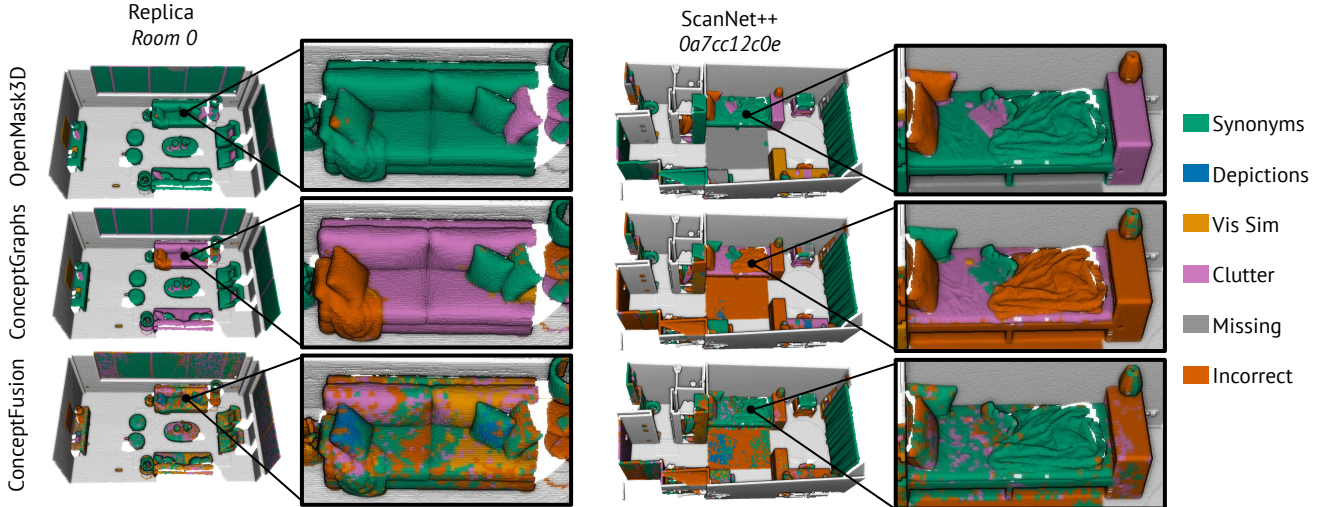


Figure 5: **Top-5 IoU results for category classification for OpenMask3D [30], ConceptGraphs [8] and ConceptFusion [12] colored by category class.** Object-centric methods that segment in 3D, like OpenMask3D (top), often miss points due to generalization or depth quality issues. Those merging 2D segments tend to merge smaller ones, leading to misclassifications (middle). Dense representations, such as ConceptFusion, produce noisier predictions due to point-level features aggregating information from various context scales. In the highly cluttered environments of ScanNet++ [37], all evaluated methods show reduced performance.

are then used to determine set inlier rates R_S and R_{DVS} as:

$$R_C = \frac{1}{|\mathcal{P}|} \sum_{p \in \mathcal{P}} \left(\frac{1}{L_C} \sum_i^{L_C} \mathbf{1}(s(r_i) = 1) \right), \quad (3)$$

where L_C denotes the number of labels per point $p \in \mathcal{P}$ for the set C (S or DVS), and $\mathbf{1}(\cdot)$ is an indicator function. In addition, we compute penalty scores that constitute inverse set ranking scores quantifying underscoring of *synonyms* and both under- and overscoring of the labels within the DVS category set. Those are defined as P_S^{\leftarrow} , P_{DVS}^{\leftarrow} , and P_{DVS}^{\rightarrow} . As formalized in Suppl. Sec. 10, they quantify the degree to which the score distribution falls short of satisfying the underlying box constraints and thus go from zero (low penalty) to one (high penalty). Lastly, we also report a mean ranking score mR , defined as:

$$mR = \frac{1}{|\mathcal{P}|} \sum_{p \in \mathcal{P}} \left(\frac{1}{L_p} \sum_i^{L_p} s(r_i) \right), \quad (4)$$

where L_p is the total number of elements in the ground truth sets S and DVS for each point p .

3.3.2 Task 2: Open-Set Object Retrieval

The object retrieval task involves segmenting object instances that correspond to a given text-based query in a similar manner to the OpenSun3D Challenge [6]. We generate queries using the synonyms in the OpenLex3D label set, along with combinations of synonyms and their associated depictions using the template “[depiction] [synonym]”.



Figure 6: **Example predictions and categories.** We show a correctly predicted label (top). *Depictions* handles cases in which the image depicted on an object is mistaken for the object itself (middle). The *visually similar* category handles reasonable but not accurate predictions (bottom).

The resulting queries include references to motifs (“polka dots duvet cover”), specific characters (“ironman portrait”) and brands (“nike athletic sneaker”). The number of queries ranges from 200 to 1,500 per scene.

For evaluation, we use the Average Precision (AP). We report AP_{50} (IoU of 50%), AP_{25} (IoU of 25%), and mAP scores averaged over the IoU range of [0.5 : 0.95 : 0.05].

4. Experiments

In this section, we present a benchmark evaluation of four state-of-the-art object-centric methods and two dense methods across two tasks: semantic segmentation and object retrieval.

4.1. Implementation

We evaluate four object-centric representations—ConceptGraphs [8], HOV-SG [33], OpenMask3D [30], and a minimal pipeline based on the findings in Kassab2024 [13]. For ConceptGraphs, we benchmark multi-view fused CLIP features (ConceptGraphs) and features derived from short GPT-generated object descriptions (ConceptGraphs (GPT)). We complement our evaluation with two dense representations: OpenScene [21] and ConceptFusion [12]. All methods take as input a set of RGB-D images and their corresponding camera poses. OpenMask3D additionally requires a mesh. The methods output either a set of features per object or dense point-wise features. Implementation details for each method are provided in Supp. Sec. 11.

We exclude floors, ceilings, and walls from our evaluation and downsample the point clouds to a resolution of 0.05 m using voxel-based downsampling. We use the ViT-H-14 CLIP backbone for all methods except OpenScene, which uses the ViT-L OpenSeg backbone.

4.2. Open-Set Semantic Segmentation

4.2.1 Top-N IoU

We report the Top-5 IoU for object-centric and dense representations in Tab. 1. The IoU at 1 and at 10 are provided in Supp. Sec. 12.2. Top down views of a selection of the output point clouds colored by category are presented in Fig. 5 for OpenMask3D, ConceptGraphs, and ConceptFusion. Examples of specific predictions and their corresponding categories are shown in Fig. 6.

As shown in Tab. 1, ConceptGraphs (GPT) is the top performing method in the *synonyms* category. The GPT prompt generates precise descriptions of the target object, which is then encoded into a highly specific text embedding. In contrast, CLIP, used by other methods, encodes both object-related and broader contextual information from the image, making it more prone to confusion due to visually similar labels or depictions. HOV-SG achieves the next best results. In general, dense methods do not effectively leverage intra-object correlations and produce noisier predictions as they use per-pixel features (Fig. 5 and Fig. 6 (middle)).

Regarding *depictions* and *visually similar* categories, OpenScene and Kassab2024 consistently yield the best results. This may stem from their distinct feature association strategies. OpenScene, unlike ConceptFusion, relies solely on per-pixel embeddings without relying on global

Dataset	Method	$S \downarrow$	$D \downarrow$	$VS \downarrow$	$C \downarrow$	$M \downarrow$	$I \downarrow$
Replica	ConceptGraphs [8]	0.41	0.01	0.11	0.24	0.02	0.22
	ConceptGraphs (GPT) [8]	0.47	0.03	0.05	0.21	0.02	0.23
	HOV-SG [33]	0.45	0.00	0.05	0.27	0.07	0.16
	Kassab2024 [13]	0.26	0.00	0.06	0.26	0.12	0.30
	OpenMask3D [30]	0.43	0.01	0.07	0.29	0.10	0.10
	ConceptFusion [12]	0.32	0.01	0.09	0.16	0.00	0.41
	OpenScene [21]	0.44	0.00	0.06	0.30	0.07	0.13
ScanNet++	ConceptGraphs [8]	0.26	0.02	0.05	0.10	0.13	0.44
	ConceptGraphs (GPT) [8]	0.43	0.01	0.04	0.11	0.13	0.28
	HOV-SG [33]	0.40	0.02	0.04	0.16	0.08	0.30
	Kassab2024 [13]	0.11	0.00	0.03	0.17	0.38	0.31
	OpenMask3D [30]	0.27	0.01	0.03	0.29	0.13	0.27
	ConceptFusion [12]	0.29	0.01	0.03	0.08	0.04	0.54
	OpenScene [21]	0.16	0.00	0.02	0.23	0.22	0.36
HM3D	ConceptGraphs [8]	0.27	0.02	0.03	0.12	0.08	0.47
	ConceptGraphs (GPT) [8]	0.45	0.01	0.04	0.11	0.09	0.31
	HOV-SG [33]	0.33	0.02	0.04	0.18	0.08	0.36
	Kassab2024 [13]	0.19	0.01	0.01	0.15	0.23	0.41
	OpenMask3D [30]	0.31	0.01	0.03	0.13	0.26	0.26
	ConceptFusion [12]	0.23	0.01	0.03	0.09	0.08	0.57
	OpenScene [21]	0.18	0.00	0.02	0.16	0.06	0.59

Table 1: **IoU Top 5 Results for Object-Centric and Dense Representations.** Where S is the IoU at synonyms, D is depictions, VS is visually similar, C is clutter, M is missing and I is incorrect. A perfectly performing method would achieve an IoU^S score approaching 1 while achieving an IoU score of 0 for all other categories.

or region-level merging strategies. Similarly, Kassab2024 selects a distinctive feature for each object using Shannon entropy without feature merging. This may preserve feature granularity and reduce classification confusion.

The *clutter* category has worse IoU results across all methods, suggesting that crop scaling and/or segmentation is critical in improving overall classification performance. This is also apparent in the *missing* category. Methods that perform initial segmentation in 3D (Kassab2024 and OpenMask3D) tend to have more missing points compared to those that segment at an image level (ConceptGraphs and HOV-SG). Kassab2024 relies solely on geometric segmentation, making it susceptible to noisy sensor data. ScanNet++ uses iPhone RGB-D depth data, which tends to be quite noisy. OpenMask3D relies on Mask3D, a fixed-class 3D segmentation model, for 3D object segmentation. This approach struggles to generalize to objects outside Mask3D’s training set, leading to missed predictions.

In general, most methods struggle with ScanNet++ and HM3D, indicating that cluttered, real-world environments still pose challenges for all approaches.

4.2.2 Set Ranking Evaluation

In Tab. 2, we report set ranking results. In general, the mean results are high, suggesting that *synonyms* tend to score higher in the predicted ranks, and that *depictions* and *visually similar* labels generally score below *synonyms*, described as the ideal ranking in Sec. 3.3.1. We observe that across all three datasets HOV-SG [33] and ConceptGraphs [8] yield consistently high mean set rank-

Dataset	Method	$mR \uparrow$	$R_S \uparrow$	P_S^{\downarrow}	$R_{DVS} \uparrow$	P_{DVS}^{\downarrow}	P_{DVS}^{\downarrow}
Replica	ConceptGraphs [8]	0.82	0.13	0.14	0.06	0.63	0.23
	ConceptGraphs (GPT) [8]	0.63	0.21	0.33	0.07	0.52	0.43
	HOV-SG [33]	0.82	0.17	0.14	0.07	0.50	0.23
	Kassab2024 [13]	0.76	0.10	0.21	0.03	0.54	0.27
	OpenMask3D [30]	0.83	0.17	0.12	0.06	0.51	0.21
	ConceptFusion [12]	0.76	0.11	0.21	0.05	0.57	0.28
	OpenScene [21]	0.85	0.16	0.10	0.05	0.53	0.21
ScanNet++	ConceptGraphs [8]	0.80	0.09	0.19	0.03	0.59	0.24
	ConceptGraphs (GPT) [8]	0.66	0.18	0.31	0.03	0.60	0.40
	HOV-SG [33]	0.84	0.15	0.14	0.04	0.64	0.19
	Kassab2024 [13]	0.72	0.05	0.26	0.01	0.60	0.30
	OpenMask3D [30]	0.79	0.12	0.19	0.02	0.57	0.25
	ConceptFusion [12]	0.74	0.10	0.26	0.02	0.63	0.30
	OpenScene [21]	0.77	0.06	0.18	0.01	0.57	0.31
HM3D	ConceptGraphs [8]	0.86	0.08	0.13	0.02	0.59	0.20
	ConceptGraphs (GPT) [8]	0.68	0.15	0.32	0.03	0.59	0.36
	HOV-SG [33]	0.88	0.12	0.11	0.02	0.59	0.19
	Kassab2024 [13]	0.80	0.06	0.19	0.01	0.62	0.26
	OpenMask3D [30]	0.86	0.10	0.12	0.02	0.56	0.20
	ConceptFusion [12]	0.78	0.07	0.20	0.02	0.61	0.27
	OpenScene [21]	0.87	0.05	0.10	0.01	0.56	0.22

Table 2: **Set Ranking Evaluation.** OpenScene [21] is evaluated using a smaller-dimensional CLIP backbone to account for its original reliance on OpenSeg [7]. ConceptGraphs (GPT) [8] relies on GPT for class predictions instead of CLIP. For mR , R_S , R_{DVS} being the mean score and the respective inlier rates, higher is better. In contrast, for the underscoring and overscoring penalties P_S^{\downarrow} , P_{DVS}^{\downarrow} , P_{DVS}^{\downarrow} , lower is better.

ing scores, while OpenScene [21] and OpenMask3D [30] achieve worse results on ScanNet++.

comparedFurthermore, we observe high R_S scores for ConceptGraphs (GPT), similar to the Top-5 IoU^S , again suggesting that the text embeddings produced from GPT captions are highly specific compared to CLIP image encodings. However, ConceptGraphs (GPT) also consistently overscores the *depictions* and *visually-similar* categories (high P_{DVS}^{\downarrow}) while also underscoring *synonyms* compared to the remaining methods (high P_S^{\downarrow}). This implies that multi-view aggregation of CLIP predictions, as executed by HOV-SG, OpenMask3D, and ConceptGraphs, better approximates the desired set distribution compared to GPT predictions, which yields rather stochastic hits resulting in high R_S scores. As demonstrated, our proposed set ranking evaluation sheds light onto non-top-performing scores and quantifies the underlying score distribution compared to the Top-N IoU metric.

4.3. Open-Set Object Retrieval

We report AP results in Tab. 3. Overall AP is low and in line with comparable benchmarks [6], highlighting the challenges of this task and the potential for improvement. OpenMask3D (with Non-Maximum Suppression and access to clean mesh inputs) leads the Replica and ScanNet++ metrics but fails to generalize to the larger HM3D scenes where ConceptGraphs is the top performing method. As observed in previous experiments, the object features of ConceptGraphs (GPT) appear to be *synonym*-focused, lowering performance on this task due to some depiction-based queries. This fact can be directly observed in Supp. Fig. 10, where we provide separate metrics for *synonym* queries and *syn-*

Dataset	Method	$mAP \uparrow$	$AP_{50} \uparrow$	$AP_{25} \uparrow$
Replica	ConceptGraphs [8]	5.86	11.32	22.39
	ConceptGraphs (GPT) [8]	5.13	10.77	18.19
	HOV-SG [33]	5.76	11.67	25.30
	Kassab2024 [13]	1.38	2.87	7.54
	OpenMask3D + NMS [30]	11.47	17.01	24.02
ScanNet++	ConceptGraphs [8]	1.45	4.36	15.27
	ConceptGraphs (GPT) [8]	1.97	5.54	13.39
	HOV-SG [33]	1.79	4.95	18.75
	Kassab2024 [13]	0.40	1.19	3.39
	OpenMask3D + NMS [30]	4.00	6.90	10.34
HM3D	ConceptGraphs [8]	5.09	8.05	11.18
	ConceptGraphs (GPT) [8]	4.80	7.75	10.76
	HOV-SG [33]	3.44	5.39	7.42
	Kassab2024 [13]	1.03	1.87	3.97
	OpenMask3D + NMS [30]	4.03	5.56	8.35

Table 3: **Object Retrieval Evaluation.** NMS stands for Non-maximum Suppression and is used to select object masks in the OpenMask3D [30] pipeline.

onym-depiction queries. For other methods, we generally observe that performance significantly increases when depiction information is part of the query. Those results emphasize the importance of a benchmark supporting queries for every object in a scene to prevent bias towards objects with prominent imagery.

For a more thorough analysis, we further report the queried object ranks in Supp. Fig. 11, with separate counts for queries with no predicted match at IoU .25. For a significant number of queries, methods fail to output predicted instances that significantly overlap with the ground truth. Properly segmenting instance geometry remains challenging for all considered methods.

5. Limitations

While our dataset offers a comprehensive set of ground truth labels across a diverse set of 3D scenes, it has certain limitations. Our label set focuses on direct labels and does not account for additional object properties such as affordances, material, and color. It is restricted to the segments provided in the original RGB-D datasets, often omitting smaller parts of a larger object such as cupboard handles or sofa cushions. Our object retrieval query set inherits the same limitations and is generated using a simple template that could warrant further investigation.

6. Conclusion

We introduced OpenLex3D, a new benchmark for open-vocabulary evaluation that captures real-world language variability across multiple levels of specificity. Our benchmark includes human-annotated labels for three RGB-D datasets—ScanNet++, Replica, and HM3D—enabling comprehensive evaluation across diverse environments. We assess the performance of both object-centric and dense representations on two key tasks: semantic segmentation and

object retrieval. Our evaluation shows that no single method performs well across both tasks, indicating that there is scope for future improvement particularly within feature fusion and segmentation strategies.

7. Acknowledgments

The authors would like to thank Ulrich-Michael, Frances, James, Maryam, and Mandolyn for their help in labeling the dataset. The work at the Université de Montréal was supported by the Natural Sciences and Engineering Research Council of Canada (NSERC) (Paull), an NSERC PGS D Scholarship (Morin) and an FRQNT Doctoral Scholarship (Morin). Moreover, this research was enabled in part by compute resources provided by Mila (mila.quebec). The work at the University of Freiburg was funded by an academic grant from NVIDIA. The work at the University of Oxford was supported by a Royal Society University Research Fellowship (Fallon, Kassab), and EPSRC C2C Grant EP/Z531212/1 (Mattamala).

References

- [1] Adel Ahmadyan, Liangkai Zhang, Artsiom Ablavatski, Jianing Wei, and Matthias Grundmann. Objectron: A large scale dataset of object-centric videos in the wild with pose annotations. In *IEEE Int. Conf. Computer Vision and Pattern Recognition*, 2021.
- [2] Dave Zhenyu Chen, Angel X Chang, and Matthias Nießner. ScanRefer: 3D Object Localization in RGB-D Scans using Natural Language. *Eur. Conf. on Computer Vision (ECCV)*, 2020.
- [3] Angela Dai, Angel X Chang, Manolis Savva, Maciej Habber, Thomas Funkhouser, and Matthias Nießner. Scannet: Richly-annotated 3d reconstructions of indoor scenes. In *IEEE Int. Conf. Computer Vision and Pattern Recognition*, pages 5828–5839, 2017.
- [4] Andrew J. Davison. FutureMapping: The Computational Structure of Spatial AI Systems. *arXiv preprint arXiv:1803.11288*, 2018.
- [5] Alexandros Delitzas, Ayca Takmaz, Federico Tombari, Robert Sumner, Marc Pollefeys, and Francis Engelmann. SceneFun3D: Fine-Grained Functionality and Affordance Understanding in 3D Scenes. In *IEEE Int. Conf. Computer Vision and Pattern Recognition*, 2024.
- [6] Francis Engelmann, Ayca Takmaz, Jonas Schult, Elisabetta Fedele, Johanna Wald, Songyou Peng, Xi Wang, Or Litany, Siyu Tang, Federico Tombari, Marc Pollefeys, Leonidas Guibas, Hongbo Tian, Chunjie Wang, Xiaosheng Yan, Bingwen Wang, Xuanyang Zhang, Xiao Liu, Phuc Nguyen, Khoi Nguyen, Anh Tran, Cuong Pham, Zhening Huang, Xiaoyang Wu, Xi Chen, Hengshuang Zhao, Lei Zhu, and Joan Lasenby. OpenSUN3D: 1st Workshop Challenge on Open-Vocabulary 3D Scene Understanding. *arXiv preprint arXiv:2402.15321*, 2024.
- [7] Golnaz Ghiasi, Xiuye Gu, Yin Cui, and Tsung-Yi Lin. Scaling open-vocabulary image segmentation with image-level labels. *Eur. Conf. on Computer Vision (ECCV)*, 2022.
- [8] Qiao Gu, Alihusein Kuwajerwala, Sacha Morin, Krishna Murthy Jatavallabhula, Bipasha Sen, Aditya Agarwal, Corban Rivera, William Paul, Kirsty Ellis, Rama Chellappa, Chuang Gan, Celso Miguel de Melo, Joshua B. Tenenbaum, Antonio Torralba, Florian Shkurti, and Liam Paull. ConceptGraphs: Open-Vocabulary 3D Scene Graphs for Perception and Planning. In *IEEE Int. Conf. Robot. Autom.*, 2024.
- [9] Jun Guo, Xiaojian Ma, Yue Fan, Huaping Liu, and Qing Li. Semantic Gaussians: Open-Vocabulary Scene Understanding with 3D Gaussian Splatting. *arXiv preprint arXiv:2403.15624*, 2024.
- [10] Felix Hill, Roi Reichart, and Anna Korhonen. SimLex-999: Evaluating Semantic Models With (Genuine) Similarity Estimation. *Computational Linguistics*, 41(4):665–695, 2015.
- [11] Daniel Honerkamp, Martin Büchner, Fabien Despinoy, Tim Welschhold, and Abhinav Valada. Language-grounded dynamic scene graphs for interactive object search with mobile manipulation. *IEEE Robot. Autom. Lett.*, 9(10):8298–8305, 2024.
- [12] Krishna Murthy Jatavallabhula, Alihusein Kuwajerwala, Qiao Gu, Mohd Omama, Tao Chen, Shuang Li, Ganesh Iyer, Soroush Saryazdi, Nikhil Keetha, Ayush Tewari, Joshua B. Tenenbaum, Celso Miguel de Melo, Madhava Krishna, Liam Paull, Florian Shkurti, and Antonio Torralba. ConceptFusion: Open-set Multimodal 3D Mapping. *Robot.: Sci. Syst.*, 2023.
- [13] Christina Kassab, Matías Mattamala, Sacha Morin, Martin Büchner, Abhinav Valada, Liam Paull, and Maurice Fallon. The Bare Necessities: Designing Simple, Effective Open-Vocabulary Scene Graphs. *arXiv preprint arXiv:2412.01539*, 2024.
- [14] Justin* Kerr, Chung Min* Kim, Ken Goldberg, Angjoo Kanazawa, and Matthew Tancik. LERF: Language Embedded Radiance Fields. In *Intl. Conf. on Computer Vision*, 2023.
- [15] Alexander Kirillov, Eric Mintun, Nikhila Ravi, Hanzi Mao, Chloé Rolland, Laura Gustafson, Tete Xiao, Spencer Whitehead, Alexander C. Berg, Wan-Yen Lo, Piotr Dollár, and Ross B. Girshick. Segment anything. In *Intl. Conf. on Computer Vision*, pages 3992–4003, 2023.
- [16] Sebastian Koch, Narunas Vaskevicius, Mirco Colosi, Pedro Hermosilla, and Timo Ropinski. Open3DSG: Open-Vocabulary 3D Scene Graphs from Point Clouds with Queryable Objects and Open-Set Relationships. In *IEEE Int. Conf. Computer Vision and Pattern Recognition*, June 2024.
- [17] Haotian Liu, Chunyuan Li, Qingyang Wu, and Yong Jae Lee. Visual Instruction Tuning. In *Intl. Conf. on Neural Information Processing Systems (NeurIPS)*, 2023.
- [18] Shiyang Lu, Haonan Chang, Eric Pu Jing, Abdeslam Boularias, and Kostas Bekris. Ovir-3d: Open-vocabulary 3d instance retrieval without training on 3d data. In *Conf. on Robot Learning (CoRL)*, pages 1610–1620. PMLR, 2023.
- [19] Dominic Maggio, Yun Chang, Nathan Hughes, Matthew Trang, Dan Griffith, Carlyn Dougherty, Eric Cristofalo, Lukas Schmid, and Luca Carlone. Clio: Real-time Task-Driven Open-Set 3D Scene Graphs. *IEEE Robot. Autom. Lett.*, 9(10):8921–8928, 2024.
- [20] George A. Miller. *WordNet: An electronic lexical database*. MIT Press, 1995.
- [21] Songyou Peng, Kyle Genova, Chiyu "Max" Jiang, An-

- drea Tagliasacchi, Marc Pollefeys, and Thomas Funkhouser. OpenScene: 3D Scene Understanding with Open Vocabularies. In *IEEE Int. Conf. Computer Vision and Pattern Recognition*, 2023.
- [22] Minghan Qin, Wanhua Li, Jiawei Zhou, Haoqian Wang, and Hanspeter Pfister. LangSplat: 3D Language Gaussian Splatting. *IEEE Int. Conf. Computer Vision and Pattern Recognition*, 2024.
- [23] Alec Radford, Jong Wook Kim, Chris Hallacy, Aditya Ramesh, Gabriel Goh, Sandhini Agarwal, Girish Sastry, Amanda Askell, Pamela Mishkin, Jack Clark, Gretchen Krueger, and Ilya Sutskever. Learning Transferable Visual Models From Natural Language Supervision. *Intl. Conf. on Machine Learning (ICML)*, 2021.
- [24] Santhosh Kumar Ramakrishnan, Aaron Gokaslan, Erik Wijmans, Oleksandr Maksymets, Alexander Clegg, John M Turner, Eric Undersander, Wojciech Galuba, Andrew Westbury, Angel X Chang, Manolis Savva, Yili Zhao, and Dhruv Batra. Habitat-Matterport 3D Dataset (HM3D): 1000 Large-scale 3D Environments for Embodied AI. In *Intl. Conf. on Neural Information Processing Systems (NeurIPS) Datasets and Benchmarks Track*, 2021.
- [25] Nils Reimers and Iryna Gurevych. Sentence-BERT: Sentence Embeddings using Siamese BERT-Networks. In *Conf. on Empirical Methods in Natural Language Processing (EMNLP)*. Association for Computational Linguistics.
- [26] Tim Rädtsch, Annika Reinke, Vivienn Weru, Minu Dietlinde Tizabi, Nicholas Heller, Fabian Isensee, Annette Kopp-Schneider, and Lena Maier-Hein. Quality Assured: Rethinking Annotation Strategies in Imaging AI. In *Eur. Conf. on Computer Vision (ECCV)*, 2024.
- [27] Johannes Lutz Schönberger and Jan-Michael Frahm. Structure-from-Motion Revisited. In *IEEE Int. Conf. Computer Vision and Pattern Recognition*, 2016.
- [28] Nur Muhammad (Mahi) Shafiullah, Chris Paxton, Lerrel Pinto, Soumith Chintala, and Arthur Szlam. Clip-fields: Weakly supervised semantic fields for robotic memory. In *Robot.: Sci. Syst.*, 2023.
- [29] Julian Straub, Thomas Whelan, Lingni Ma, Yufan Chen, Erik Wijmans, Simon Green, Jakob J. Engel, Raul Mur-Artal, Carl Ren, Shobhit Verma, Anton Clarkson, Mingfei Yan, Brian Budge, Yajie Yan, Xiaqing Pan, June Yon, Yuyang Zou, Kimberly Leon, Nigel Carter, Jesus Briales, Tyler Gillingham, Elias Mueggler, Luis Pesqueira, Manolis Savva, Dhruv Batra, Hauke M. Strasdat, Renzo De Nardi, Michael Goesele, Steven Lovegrove, and Richard Newcombe. The Replica Dataset: A Digital Replica of Indoor Spaces. *arXiv preprint arXiv:1906.05797*, 2019.
- [30] Ayça Takmaz, Elisabetta Fedele, Robert W. Sumner, Marc Pollefeys, Federico Tombari, and Francis Engelmann. OpenMask3D: Open-Vocabulary 3D Instance Segmentation. In *Intl. Conf. on Neural Information Processing Systems (NeurIPS)*, 2023.
- [31] Nikolaos Tsagkas, Oisín Mac Aodha, and Chris Xiaoxuan Lu. VI-fields: Towards language-grounded neural implicit spatial representations. *arXiv preprint arXiv:2305.12427*, 2023.
- [32] Austin T. Wang, ZeMing Gong, and Angel X. Chang. ViGiL3D: A linguistically diverse dataset for 3d visual grounding. *arXiv preprint arXiv:2501.01366*, 2024.
- [33] Abdelrhman Werby, Chenguang Huang, Martin BÜchner, Abhinav Valada, and Wolfram Burgard. Hierarchical Open-Vocabulary 3D Scene Graphs for Language-Grounded Robot Navigation. *Robot.: Sci. Syst.*, 2024.
- [34] Yanmin Wu, Jiarui Meng, Haijie Li, Chenming Wu, Yahao Shi, Xinhua Cheng, Chen Zhao, Haocheng Feng, Errui Ding, Jingdong Wang, and Jian Zhang. OpenGaussian: Towards Point-Level 3D Gaussian-based Open Vocabulary Understanding. *arXiv preprint arXiv:2406.02058*, 2024.
- [35] Zhengyuan Yang, Linjie Li, Kevin Lin, Jianfeng Wang, Chung-Ching Lin, Zicheng Liu, and Lijuan Wang. The Dawn of LMMs: Preliminary Explorations with GPT-4V(ision). *arXiv preprint arXiv:2309.17421*, 2023.
- [36] Sriram Yenamandra, Arun Ramachandran, Karmesh Yadav, Austin Wang, Mukul Khanna, Theophile Gervet, Tsung-Yen Yang, Vidhi Jain, Alexander William Clegg, John Turner, Zsolt Kira, Manolis Savva, Angel Chang, Devendra Singh Chaplot, Dhruv Batra, Roozbeh Mottaghi, Yonatan Bisk, and Chris Paxton. HomeRobot: Open Vocabulary Mobile Manipulation. *arXiv preprint arXiv:2306.11565*, 2023.
- [37] Chandan Yeshwanth, Yueh-Cheng Liu, Matthias Nießner, and Angela Dai. ScanNet++: A High-Fidelity Dataset of 3D Indoor Scenes. In *Intl. Conf. on Computer Vision*, 2023.
- [38] Zihan Zhu, Songyou Peng, Viktor Larsson, Weiwei Xu, Hujun Bao, Zhaopeng Cui, Martin R. Oswald, and Marc Pollefeys. NICE-SLAM: Neural Implicit Scalable Encoding for SLAM. In *IEEE Int. Conf. Computer Vision and Pattern Recognition*, 2022.

OpenLex3D: A New Evaluation Benchmark for Open-Vocabulary 3D Scene Representations

Supplementary Material

8. Datasets - Further Details

In this appendix we provide details about the scenes selected from the parent datasets and their type (Tab. 4). Our goal was to include a diverse range of environments, covering various home and living spaces of different scales, as well as office and laboratory spaces.

Dataset	Scene ID	Scene Type
ScanNet++	0a76e06478	Bedroom
	0a7cc12c0e	Studio apartment
	1f7cbbdde1	Studio apartment
	49a82360aa	Living area & office
	4c5c60fa76	Lab room
	8a35ef3cfe	Living area & kitchen
	c0f5742640	Kitchen
jd361ab85f	Office	
HM3D	00824-Dd4bFSTQ8gi	Single-story home
	00829-QaLdnwvtxbs	Single-story home
	00843-DYehNKdT76V	Two-story home
	00847-bCPU9suPUw9	Three-story home
	00873-bxsVRursffK	Two-story home
	00877-4ok3usBNeis	Two-story home
	00890-6s7QHgap2fW	Two-story home
Replica	office0	Meeting room
	office1	Common room
	office2	Meeting room
	office3	Meeting room
	office4	Meeting room
	room0	Living room
	room1	Bedroom
room2	Dining room	

Table 4: **Full list of chosen scenes and scene types.** The scenes are from a variety of environments including studio apartments and multi-storey homes, offices, meeting rooms, and labs.

9. Labeling Instructions

The instructions provided to the human annotators were as follows:

You will be presented with multiple views of an object. We removed the background in the top left view to highlight the relevant object. Please label the object according to the following three category system:

Synonyms. Assign the most accurate label for the object, along with any closely related synonyms. For example:

- sofa, couch, settee
- screen, monitor, computer
- glasses, spectacles

For bottles and containers, consider adding both the content and a reference to the container. For example: ketchup, ketchup bottle

Depictions. If the object features a distinct pattern, image, or design of another object or concept, label it accordingly. For example, if you see a painting, figurine or toy representing a cat or a book on cats, you might use:

- cat

You can also add to this category legible words or brands.

Visually Similar Objects. Identify objects that are not synonyms but appear visually similar to the highlighted object. Consider objects of similar color or shape. Visually similar labels should be wrong, but have an understandable visual connection with the displayed object.

Examples corresponding to the objects mentioned in Synonyms might include:

- chair, armchair

- television

- sunglasses, goggles

Notes:

- Please separate each input with a comma (,).

- You can use multiple words as a label. Please separate words belonging to the same label with a space (). For example “coffee mug” or “ice cream”.

- You are encouraged to input as many appropriate labels as you can think of for each level.

- If you cannot think of any appropriate labels for any level, simply leave that level blank.

- You can leave all levels blank.

Additional Notes for ScanNet++ Scenes:

- Some crops may show a magenta mask to protect privacy. Please ignore it.

- If a crop covers multiple objects, please list them separately. If there are too many objects, focus on the main ones.

- If the relevant object(s) is unclear because the crops are too blurry or showing different objects, please leave all the fields blank.

10. Additional Details on Set Ranking Metric

In the following, we formalize the left and right box constraint penalties which were mentioned in Sec. 3.3.1. As the *synonyms* are considered the primary target-rank set, we only need to consider a violation of its right box constraint

due to potential underscoring of *synonyms*, which is formalized as:

$$R_S^{\text{right}} = 1 - \frac{1}{|\mathcal{P}|} \sum_{p \in \mathcal{P}} \left(\frac{1}{L_S} \sum_i^{L_S} \left(1 + \min \left(0, \frac{r_i - b_i^S}{b_i^S} \right) \right) \right), \quad (5)$$

where L_S represents the set of synonym labels of each object $p \in \mathcal{P}$. Similarly, we compute the left and right box-constraint scores for the *DVS* category set as

$$R_{DVS}^{\text{left}} = \frac{1}{|\mathcal{P}|} \sum_{p \in \mathcal{P}} \left(\frac{1}{L_{DVS}} \sum_i^{L_{DVS}} \left(1 - \max \left(0, \frac{r_i - b_r^{DVS}}{L - b_r^{DVS}} \right) \right) \right), \quad (6)$$

$$R_{DVS}^{\text{right}} = \frac{1}{|\mathcal{P}|} \sum_{p \in \mathcal{P}} \left(\frac{1}{L_{DVS}} \sum_i^{L_{DVS}} \left(1 + \min \left(0, \frac{r_i - b_l^{DVS}}{b_l^{DVS}} \right) \right) \right) \quad (7)$$

$$(8)$$

where L_{DVS} represents the set of *DVS* labels of each object $p \in \mathcal{P}$. Since those scores measure normalized rank similarity rather than quantifying a penalty, we inverse them as follows:

$$P_S^{\leftarrow} = 1 - R_S^{\text{right}}, \quad (9)$$

$$P_{DVS}^{\leftarrow} = 1 - R_{DVS}^{\text{left}}, \quad (10)$$

$$P_{DVS}^{\rightarrow} = 1 - R_{DVS}^{\text{right}} \quad (11)$$

Thus, P_S^{\leftarrow} quantifies the *synonym* underscoring penalty, P_{DVS}^{\leftarrow} quantifies the *DVS* overscoring penalty, whereas P_{DVS}^{\rightarrow} quantifies the *DVS* underscoring penalty.

11. Implementation Details

Kassab2024. We follow the execution of the pipeline described in Kassab et al. [13]. We chose intervals of 25 frames, using region-growing parameters of 100 considered neighbors, a smoothness threshold of 0.05 radians, a curvature threshold of 1, and a tree-based search method. The entropy was calculated using the 100-label Replica prompt list, as described in the paper.

ConceptGraphs. We ran ConceptGraphs [8] with a stride of 10 frames and at a similarity threshold of 0.75.

ConceptGraphs (GPT). As in the original ConceptGraphs paper, we rely on a VLM to extract object captions from multiple views. We streamline captioning by providing `gpt-4o` with the 4 best object views (based on SAM segment area) and prompt it to give a succinct description of the central object:

Dataset	# of Scenes	Unique Labels	Labels per Object	Min # of Labels per Object	Max # of Labels per Object	Ambiguous Objects
Replica	8	361	14	1	28	3
ScanNet++	8	771	12	1	27	1
HM3D	7	648	8	1	24	31

Table 5: **Analysis of the category labels in each dataset (averaged per scene).** Each scene contains a diverse range of unique labels for all categories. HM3D has a high number of difficult-to-classify objects.

You are a helpful assistant that describes objects in a single word. You will be provided with up to 4 views of the same object. Describe the object with a few words. You should generally use a single word, but you can use more than one if needed (e.g., ice cream, toilet paper).

We embed the resulting description with CLIP and use this instead of the standard ConceptGraphs features. The representation is otherwise identical to ConceptGraphs.

HOV-SG. We run the publicly-available HOV-SG [33] pipeline using a stride of 10 frames and its sequential merge paradigm. All other parameters remain unchanged.

OpenMask3D. OpenMask3D [30] was executed at intervals of 10 frames. For the open-set semantic segmentation task, points belonging to multiple masks, the mask with the highest score was chosen for that point. For the open-set object retrieval task, non-maximum suppression (with an IoU threshold of 0.50) was applied to all masks. All the resultant masks were then used for AP calculation.

ConceptFusion. We ran ConceptFusion [12] with a default stride of 10 frames, increasing it as needed for larger scenes to fit in memory. We used the SAM version and default parameters from the repository.

OpenScene. OpenScene [21] was executed at intervals of 10 frames. For evaluation, we use the multi-view 2D fused features, as they better align with the other methods.

12. Experiments

12.1. Label Analysis

Tab. 5 provides a breakdown of the number and variety of labels present in each dataset. On average, each scene contains between 300 and 800 unique labels, with up to 14 labels per object across the categories. We define ambiguous objects as those with unclear ground truth masks, making them difficult to label. Among the three datasets, HM3D had the highest number of ambiguous objects.

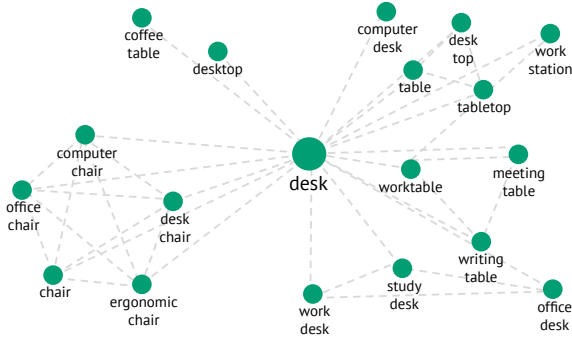


Figure 7: A subset of the labels connected to the word *desk* in the OpenLex3D synonym label set. Our labels encompass the diversity of real-world object names, allowing more realistic evaluation of open-vocabulary representations.

The labels captured in the dataset encompass a broad range of semantically similar terms, such as “pillow” and “cushion”, or “sofa” and “couch”. By incorporating this large range of synonyms, our benchmark aligns well with real-world variability in object naming. This allows for a deeper level analysis and evaluation of open-vocabulary representations. We show a visual example of a subset of words connected to the label *desk* in Fig. 7.

12.2. Top N IoU - Further Results

We present Top 1 and Top 10 quantitative IoU results in Tab. 6. We also show qualitative comparisons in Fig. 8 for OpenMask3D and ConceptFusion.

As N increases IoU^S increases, and IoU^I decreases with all other categories experiencing minor changes of approximately 0.01. Relaxing the metric to $N = 5$ helps mitigate against minor inconsistencies in the ground truth data, particularly when the correct label for the target object is absent due to the large variety of labels. For example, in Fig. 8, OpenMask3D predicts “smart board screen” for the top 1 prediction which is categorized as *clutter*. This occurs because a nearby screen is labeled “smart board screen”, while the target object is not. By considering the top 5 predictions, the correct label, “smart board” is found, re-categorizing the prediction as a *synonym*.

By increasing N we account for ambiguities in language descriptions, while also ensuring that entirely incorrect predictions remain unchanged, as demonstrated for ConceptFusion in Fig. 8 (bottom). We select $N = 5$ as an optimal balance between accommodating label ambiguity and preventing the metric from being overly permissive, which could lead to incorrect predictions being classified as *synonyms* or other categories. Additional qualitative results at $N = 5$ are shown in Figure 9.

N	Dataset	Method	S ↓	D ↓	VS ↓	C ↓	M ↓	I ↓
	Replica	ConceptGraphs	0.18	0.01	0.06	0.13	0.02	0.61
		ConceptGraphs (GPT)	0.37	0.03	<u>0.03</u>	0.14	0.02	<u>0.41</u>
		HOV-SG	0.25	0.01	<u>0.03</u>	0.22	0.07	0.42
		Kassab2024	0.13	0.00	0.04	0.28	0.11	0.45
		OpenMask3D	<u>0.27</u>	0.00	0.02	0.26	0.10	0.35
		ConceptFusion	0.18	0.01	0.06	0.13	0.02	0.61
	1	OpenScene	0.20	0.00	0.04	0.20	0.07	0.49
		ConceptGraphs	0.12	0.01	0.02	<u>0.05</u>	0.13	0.68
		ConceptGraphs (GPT)	0.33	<u>0.01</u>	0.03	0.08	0.13	0.42
		HOV-SG	<u>0.2</u>	0.02	0.03	0.09	0.08	0.59
		Kassab2024	0.05	0.00	0.01	0.08	0.38	0.49
		OpenMask3D	0.15	<u>0.01</u>	0.01	0.17	0.13	<u>0.53</u>
	10	ConceptFusion	0.15	<u>0.01</u>	0.02	0.04	0.04	0.74
		OpenScene	0.07	0.00	0.01	<u>0.11</u>	0.22	0.59
		ConceptGraphs	0.10	0.01	0.01	0.04	<u>0.08</u>	0.75
		ConceptGraphs (GPT)	0.32	0.00	0.03	0.09	0.09	0.47
		HOV-SG	<u>0.13</u>	0.01	0.02	0.07	0.08	0.69
		Kassab2024	0.08	0.00	<u>0.01</u>	0.05	0.22	0.65
	Replica	OpenMask3D	0.15	0.00	<u>0.01</u>	0.07	0.29	0.48
		ConceptFusion	0.09	0.01	<u>0.01</u>	0.03	0.08	0.79
		OpenScene	0.07	0.00	0.00	<u>0.04</u>	0.06	0.83
		ConceptGraphs	<u>0.52</u>	0.01	0.12	<u>0.23</u>	<u>0.02</u>	0.11
		ConceptGraphs (GPT)	<u>0.52</u>	0.02	0.04	<u>0.23</u>	<u>0.02</u>	0.17
		HOV-SG	0.51	0.00	0.07	0.27	0.07	0.08
	10	Kassab2024	0.33	0.00	0.08	0.24	0.12	0.22
		OpenMask3D	0.51	0.01	0.07	0.26	0.10	0.06
		ConceptFusion	0.40	0.01	0.10	0.20	0.00	0.29
		OpenScene	0.55	0.00	<u>0.05</u>	0.29	0.07	0.04
		ConceptGraphs	0.35	0.02	0.06	0.12	0.13	0.32
		ConceptGraphs (GPT)	0.48	0.01	0.04	<u>0.11</u>	0.13	<u>0.23</u>
	ScanNet++	HOV-SG	0.48	0.01	0.05	0.16	0.08	0.22
		Kassab2024	0.15	0.00	0.03	0.19	0.38	0.25
		OpenMask3D	0.35	0.01	0.04	0.31	0.13	0.17
		ConceptFusion	0.35	0.01	0.04	0.09	0.04	0.46
		OpenScene	0.21	0.00	0.03	0.29	0.22	0.25
		ConceptGraphs	0.34	0.02	0.04	0.16	0.08	0.35
	HM3D	ConceptGraphs (GPT)	0.53	0.00	0.03	0.12	0.09	<u>0.23</u>
		HOV-SG	0.43	0.02	0.09	0.20	0.08	<u>0.23</u>
		Kassab2024	0.25	0.01	0.02	0.17	0.23	0.33
		OpenMask3D	0.42	0.00	0.02	<u>0.13</u>	0.29	0.13
		ConceptFusion	0.29	0.01	0.03	0.10	0.08	0.48
		OpenScene	0.27	0.00	0.02	0.25	0.06	0.39

Table 6: **IoU Top 1 and 10 Results for Object-Centric and Dense Representations.** Where S is synonyms, D is depictions, VS is visually similar, C is clutter, M is missing and I is incorrect.

12.3. Object Retrieval - Query Analysis

We provide additional details on the number of *synonym*-only queries and queries formed from both a *synonym* and a *depiction* in the object retrieval task in Tab. 7. The number of queries ranges from 200 up to 1500 per scene, as opposed to previous open-vocabulary evaluations, allowing comprehensive evaluation.

12.4. Object Retrieval - Further Results

We provide additional context for the object retrieval experiment in Fig. 10 and Fig. 11.

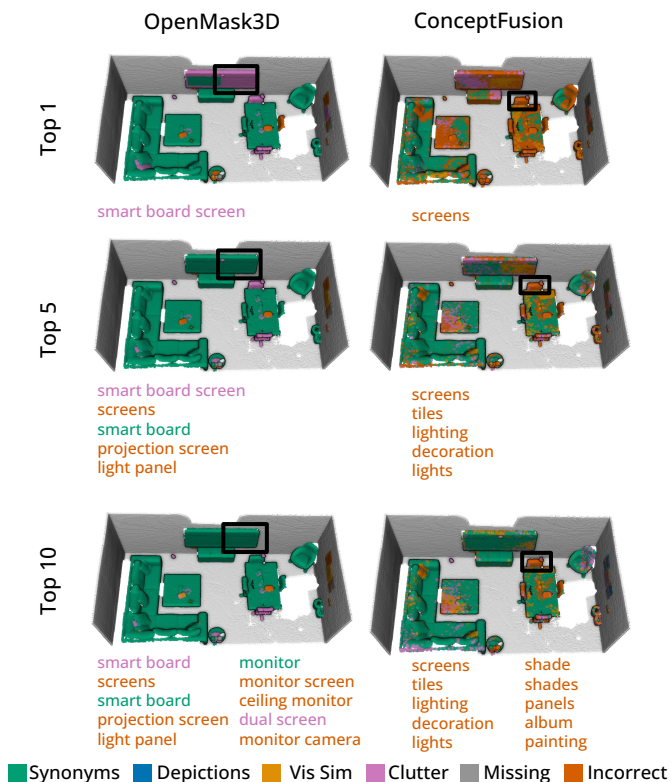


Figure 8: **Top 1, 5 and 10 Comparison for OpenMask3D [30] and ConceptFusion [12] on Replica [29] Office 2.** Increasing N allows for ambiguities in semantically similar labels (top) while also ensuring that incorrectly predicted labels remain incorrect (bottom).

Dataset	Scene ID	# of S Queries	# of $S + D$ Queries	Total Queries
ScanNet++	0a76e06478	356	1068	1424
	0a7cc12c0e	377	169	546
	1f7cbbdde1	629	782	1411
	49a82360aa	433	409	842
	4c5c60fa76	633	864	1497
	8a35ef3cfe	303	532	835
	c0f5742640	414	488	902
fd361ab85f	250	137	387	
HM3D	00824	340	173	513
	00829	372	293	665
	00843	367	98	465
	00847	424	128	552
	00873	623	945	1568
	00877	569	518	1087
Replica	00890	624	216	840
	office0	195	211	406
	office1	163	70	233
	office2	208	87	295
	office3	211	112	323
	office4	176	122	298
	room0	236	373	609
	room1	164	93	257
room2	165	122	287	

Table 7: **Query Analysis.** S refers to *synonyms* only queries, while $S + D$ refers to queries comprised of both *synonyms* and *depictions* labels.

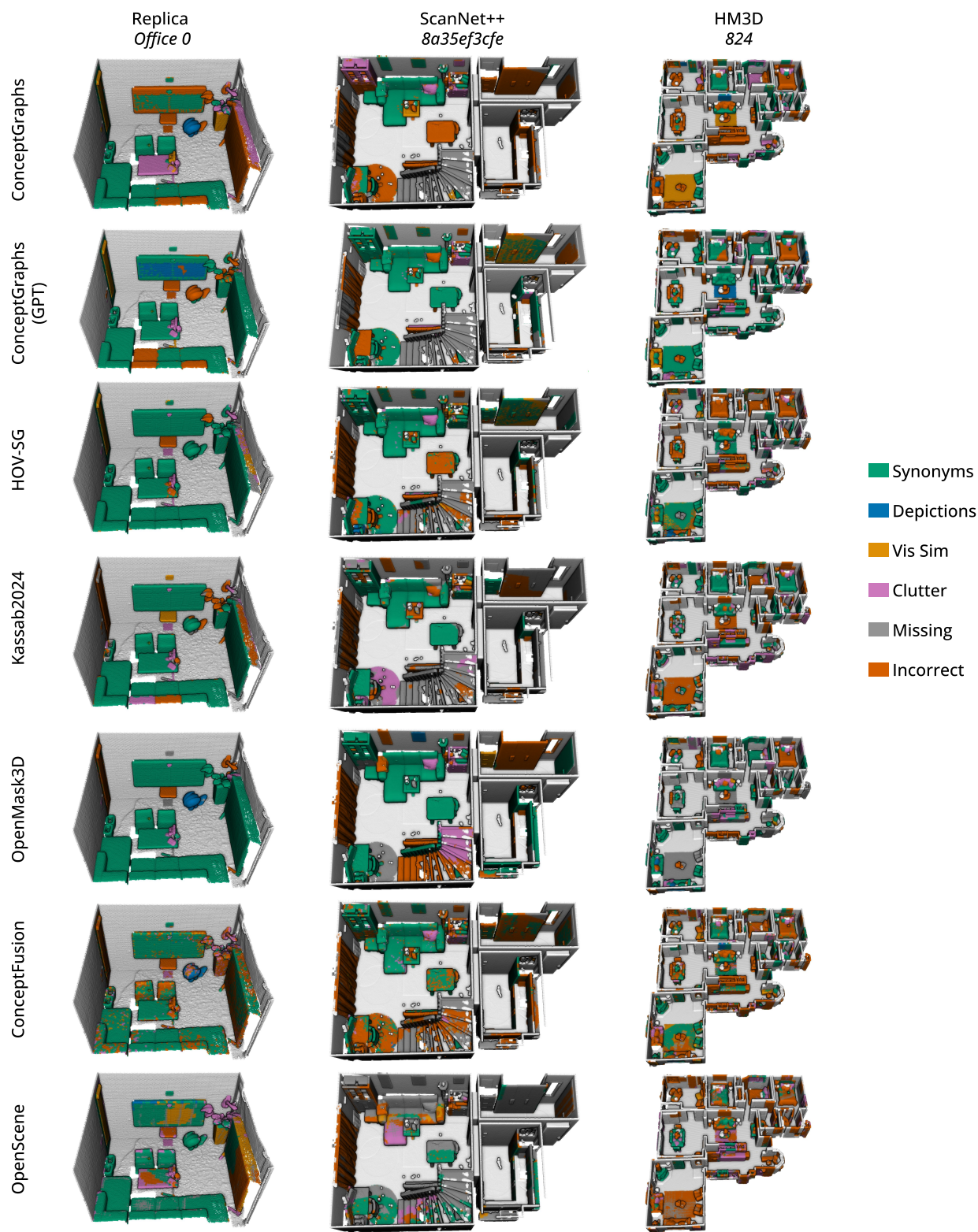


Figure 9: **Qualitative Top 5 IoU Results.** We show results from all assessed methods on a selected scene from each dataset. The scenes range from small-scale reconstructed environments (Replica [29]) to large-scale cluttered home environments (HM3D [24]).

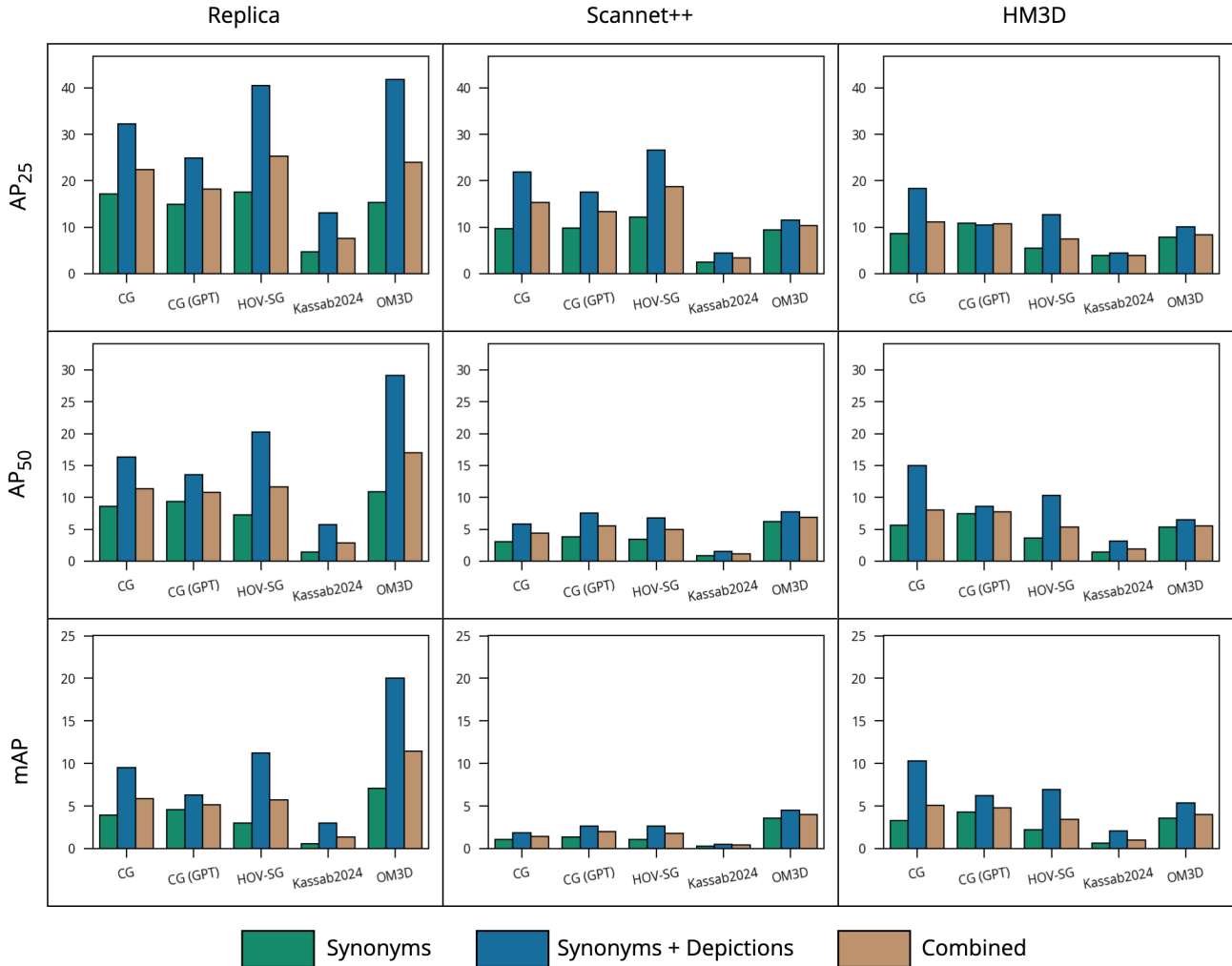


Figure 10: **AP by Category.** We break down the query metrics to distinguish *synonym*-only queries and queries formed from both a *synonym* and a *depiction*. CG, CG (GPT), and OM3D respectively refer to ConceptGraphs [8], ConceptGraphs (GPT) [8], and OpenMask3D [30]. Depictions tend to be more specific and feature salient concepts that are likely unique in the scene (e.g., a fisherman on a pillow in a Replica [29] room). We posit that this explains the significant gap in performance in favor of depiction-based queries. This experiment underscores the importance of a benchmark that provides queries for every object in a scene.

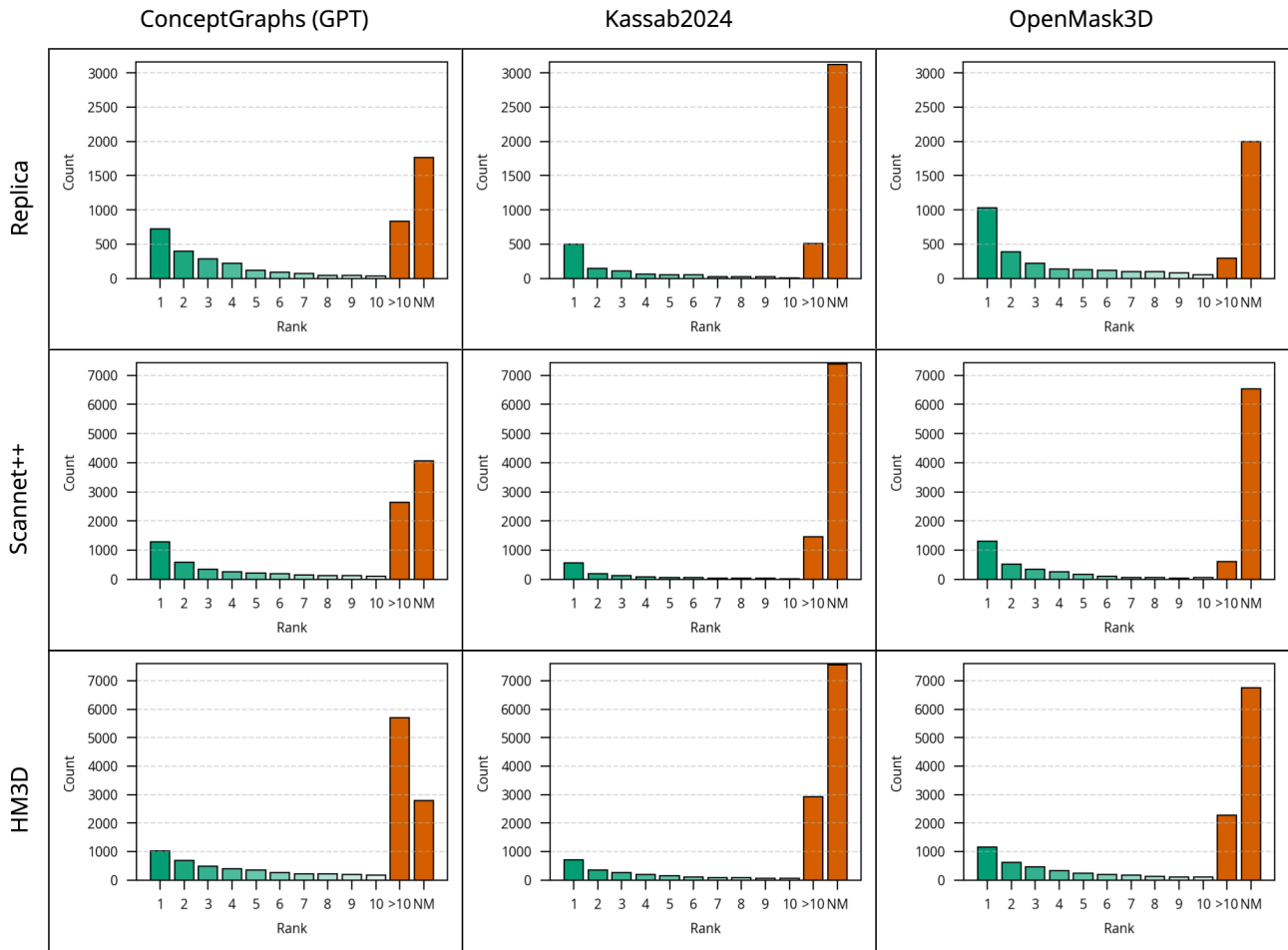


Figure 11: **Query Rank Counts.** We embed each OpenLex3D query and rank the predicted objects of each method based on feature similarity. If the target ground truth instance has an IoU of at least 0.25 with a predicted instance, we report the corresponding predicted rank. Otherwise, the query counts as “No Match” (NM). Queries with a rank of 10 or above are grouped together. The high number of unmatched queries confirms that most methods still struggle with the geometric aspect of the task and fail to segment instances that sufficiently overlap with the ground truth.